

RSC Advances

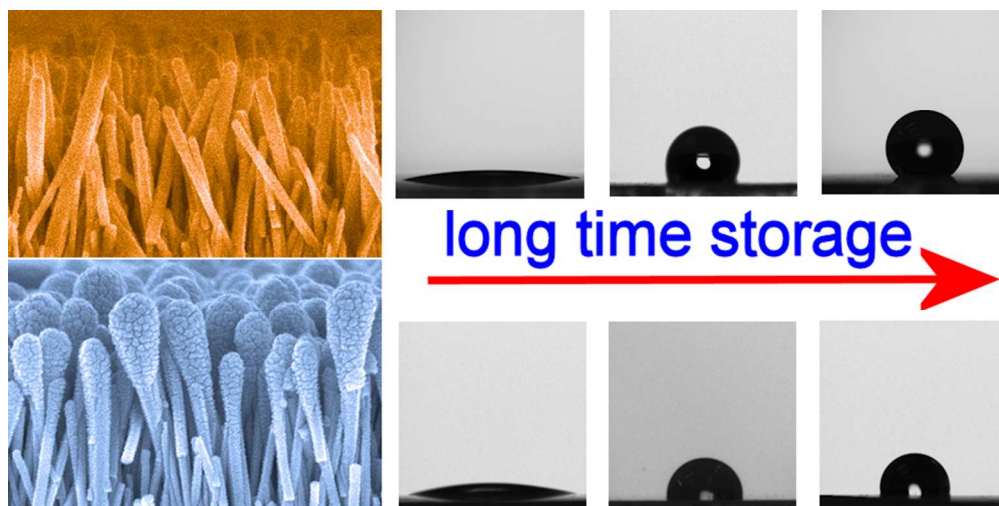


This is an *Accepted Manuscript*, which has been through the Royal Society of Chemistry peer review process and has been accepted for publication.

Accepted Manuscripts are published online shortly after acceptance, before technical editing, formatting and proof reading. Using this free service, authors can make their results available to the community, in citable form, before we publish the edited article. This *Accepted Manuscript* will be replaced by the edited, formatted and paginated article as soon as this is available.

You can find more information about *Accepted Manuscripts* in the [Information for Authors](#).

Please note that technical editing may introduce minor changes to the text and/or graphics, which may alter content. The journal's standard [Terms & Conditions](#) and the [Ethical guidelines](#) still apply. In no event shall the Royal Society of Chemistry be held responsible for any errors or omissions in this *Accepted Manuscript* or any consequences arising from the use of any information it contains.



80x39mm (300 x 300 DPI)

Cite this: DOI: 10.1039/c0xx00000x

www.rsc.org/xxxxxx

ARTICLE TYPE

TiO₂/ZnO nanocomposite, ZnO/ZnO bi-level nanostructure and ZnO nanorod arrays: microstructure and time-affected wettability change in ambient conditions

Yangsi Liu,^{*a} Weiwei Chen,^b Shanghai Wei^a and Wei Gao^a

⁵ Received (in XXX, XXX) Xth XXXXXXXXXX 20XX, Accepted Xth XXXXXXXXXX 20XX
DOI: 10.1039/b000000x

Wettability is an important property of surface and interface. Understanding the wetting behavior of semiconductors and the relationship with their microstructures has aroused much interest because of the great advantages given to various functional applications. Herein, we report the fabrication of ZnO based nanoarrays, including ZnO nanorods, TiO₂/ZnO nanocomposites and ZnO/ZnO bi-level nanostructures, by hydrothermal growth and physical vapor deposition, and their wettability conversion. The ZnO matrix arrays consist of many hexagonal wurtzite nanorods. The microstructure and morphology of the TiO₂/ZnO and ZnO/ZnO nanostructure arrays were studied. The wettability conversion of these ZnO based nanoarrays in the ambient conditions was monitored during a long period of time. It was found that their surfaces transitioned from hydrophilic to hydrophobic without any external stimulation. The morphological features and the surface chemical changes, such as replacing of hydroxyl groups and adding of organic contaminants, would affect the wettability behavior. Our results also demonstrated the possibility of slowing the loss of hydrophilic states by TiO₂ decoration.

1. Introduction

Wettability is one of the essential properties of solid material surface and of great importance to the interface between liquid and solid. Generally, according to the water contact angle (CA) on a solid surface, surfaces can be defined as hydrophobic (CA > 90°) or hydrophilic (CA < 90°).¹ It is believed that the wettability is governed by both the inherent chemical composition and the geometrical structure of solid surfaces.²⁻⁴

Controlling surface wettability is highly demanded for a wide range of chemical, electronic devices, biological, agricultural industries, and everyday life.^{1, 5} On the other hand, the wetting process of solid material surface by liquids is of great interest in both fundamental studies and practical applications. For instance, the developments of self-cleaning surfaces,^{6, 7} antifogging coatings,⁸ microfluidics,⁹ sensors¹⁰ and the biocompatibility of solid surfaces¹¹, are all related to the wetting process.

Recently, there has been enthusiasm in studying the wetting behaviors of metal oxide semiconductors, such as ZnO,^{1, 2, 12-14} SiO₂,¹⁵ and TiO₂.¹⁶ Among these semiconductors, ZnO has drawn a lot of attention on its special electrical, optical, and catalytic properties due to its direct wide band gap (3.37 eV), large exciton binding energy (60 meV) at room temperature and transparency for visible light.¹⁷⁻¹⁹

Many researches have been focused on controlling ZnO surfaces to obtain the desirable functional properties, either hydrophobicity or hydrophilicity, or even superhydrophobicity (CA > 150°) and superhydrophilicity (CA > 5°). The special

wettability can be usually achieved by applying external stimuli and treatments such as UV light illumination,^{13, 20} chemical modification,^{21, 22} electric field,²³ plasma,^{12, 22} and thermal treatment.²⁴

However, studies on the time-affected wettability change of ZnO nanostructures are quite limited. Mondal *et al* reported the reversible switching from a superhydrophobic to a superhydrophilic state of the ZnO nano-columnar thin film by UV irradiation; and they observed that on keeping the film under ambient conditions for a certain time, the hydrophilic as-prepared surface became hydrophobic.¹³ Zhu *et al* obtained the superhydrophobic ZnO nanorod-arrayed surface by *n*-octadecanoic acid modification, and indicated that the as-prepared fresh ZnO surface showed a hydrophilic behavior without any chemical modification.²¹ They compared this result with the superhydrophobic ZnO surface from Feng *et al*, and attribute the difference to the time of testing since they measured the wettability immediately after the sample fabricated, while Feng *et al* stored the ZnO nanorod films in dark for several days.²⁵ Although the wettability conversion of ZnO surfaces in the air has been mentioned, there is no explanation for this phenomenon in these literatures; and the spontaneous change of the surface wetting property during long-term period under ambient conditions is rarely reported.

In the present study, we prepared the ZnO nanorod (ZNR) arrays by a benign aqueous solution method, and used magnetron sputtering of TiO₂ and ZnO to modify ZNR arrays to obtain more complex arrays composed of “core-shell” nanostructures. While

the microstructure of ZnO based nanoarrays was studied, we also monitored the CA on their surface during a long period of time when they were placed in dark under ambient temperature. During the sample storage, no external stimuli or other treatment was conducted to the surface, so the variation of wettability was totally in a “self-managed” process. The mechanism and the reasons for the time-affected wettability alteration and the relationship with their microstructures were investigated. The main objective to this work is to gain the understanding of surface chemistry variation and wettability transition of semiconductor nanostructure, which would enrich our knowledge of design, storage and applications of these materials.

2. Experimental

2.1 Sample preparation

2.1.1. Formation of ZnO nanorod arrays

All chemicals of analytical grade and de-ionized (DI) water were used throughout this study. The hydrothermal method for growing immobilized ZnO nanorods has been described in our previous report.²⁶ In brief, clean glass slides were pre-coated with ZnO seed layers by magnetron sputtering to get the ZNRs substrates. An aqueous solution containing 25 mM zinc nitrate ($\text{Zn}(\text{NO}_3)_2 \cdot 6\text{H}_2\text{O}$, 98%) and hexamethylenetetramine (HMT) ($\text{C}_6\text{H}_{12}\text{N}_4$, 99%) with an equal molar ratio was prepared as the reactant resource. The substrates were immersed into a sealable glass jar with the reactant solution and kept face-down at 95°C for 4 h. Afterwards, the glass slides were rinsed and dried, and kept in pertri dishes in the dark.

2.1.2 Fabrication of TiO_2/ZnO and ZnO/ZnO nanostructure arrays

The complex nanoarrays were synthesised by depositing a layer of TiO_2 or ZnO on the surface of ZNRs using magnetron sputter. The ZNRs were mounted into a working chamber installed with the sputtering target (TiO_2 or ZnO, 99.99%). The unit was evacuated until the background vacuum pressure was lower than 6.7×10^{-4} Pa. Argon gas with a flow rate of 10 sccm and a pressure of 1.33 Pa was used as the working gas. The target was then activated by a DC current of 0.25 A. The deposition was performed for 2 h and 4 h by TiO_2 target and ZnO target. The ZnO based nanoarrays were named after their composition and preparation time, e.g. 4TZ for TiO_2 decorated ZNRs by 4 h deposition using TiO_2 target, 2TZ for TiO_2 decorated ZNRs by 2 h deposition using TiO_2 target and 2ZZ for ZnO decorated ZNRs by 2 h deposition using ZnO target.

2.2 Sample characterization

The crystal structure of the ZnO based nanoarrays was identified by X-ray diffraction (XRD, Philips X'Pert MPD) using Cu $K\alpha$ radiation. Their morphology and microstructure were characterized by a field-emission gun scanning electron microscope (FEG-SEM, FEI XL-30S), transmission electron microscope (TEM, Philips CM12 120 KV) and a high resolution transmission electron microscope (HRTEM, Philips Tecnai G² F20, 200 KV). The chemical composition of 4TZ was analysed with energy dispersive spectroscopy (EDS) equipped on SEM. Raman scattering (Renishaw System 1000) and X-ray photoelectron spectroscopy (XPS, PHI Quantera-II SXM) were

employed to study the microstructures and chemical states of the TiO_2 outer layers of 4TZ.

2.3 Wettability measurement

The surface wettability of the ZnO based nanoarrays was evaluated by water contact angle measured on a contact-angle goniometer (KSV CAM 101). A Milli-Q water droplet was gently placed on the surface of the samples using a microsyringe. To obtain a stable contact angle, all measurements were conducted 30 s after positioning the water droplet. Each contact angle was repeated at least five times at different positions and the mean value was calculated. The wettability of each sample was measured intermittently after different storage times.

3. Results and discussion

3.1 Morphology and composition

The morphology of the ZnO based nanoarrays are illustrated in Figure 1. The top section views disclose the distribution of the nanostructures of each sample. The nanorod structures are spread uniformly and closely packed into large arrays. The size of tips increases in tandem with decreasing density from ZNRs to 2ZZ (Fig. 1a-d).

The ZnO nanorods possess the similar diameter through their entire bodies and the majority of them are vertical to the substrates as shown in the cross section views of Fig. 1e-h. The nanorod based structures from 2TZ, 4TZ and 2ZZ are also perpendicularly arrayed, but the rod bodies have enlarged from the bottom to the top to various extents. Fluffy matters were covered on the top surface and upper bodies of 2TZ with many tiny cracking blocks. This becomes more obvious for 4TZ, which looks like a cotton swab array with bigger tops than 2TZ. 2ZZ exhibits a lollipop configuration, in which the narrow nanorods' lower bodies are supporting the much thicker upper parts compared with ZNRs, 2TZ and 4TZ. Not many cracks can be seen, indicating the good compatibility of the deposition with the original nanorods. The gaps within the arrays become narrower from ZNRs to 2TZ and 4TZ, and even closed in 2ZZ.

The elemental composition along the TiO_2/ZnO nanocomposite bodies was detected by EDS. Three adjacent areas (500 nm \times 500 nm) were selected from the top to the bottom of 4TZ as shown in Figure 2. In the EDC spectra, the highest Zn peaks indicate the nanoarrays are based on the ZnO nanorod matrixes, and the Ti peaks come from the TiO_2 deposition. Apart from Si of the glass substrates and Pt from pre-SEM coating, O is the only element left, proving the purity of 4TZ.

From area #1 to area #2 and to area #3, the intensity of Zn peaks increases, the Ti peaks reduce and the atomic ratio of Ti/Zn decreases accordingly from 0.864 to 0.265 and to 0.113, implying that most of TiO_2 are concentrated on the top surfaces and some of them attached on the upper parts, but a little has reach the bottom. This is related to the feature of magnetron sputtering. The target materials arrive on the top and the upper side surfaces first, and gradually the space for passing through would be obstructed. Therefore, more TiO_2 is accumulated on the top parts of the ZnO nanorods with prolongation of the deposition time and make themselves into a cotton swab-like structure as shown in the SEM images.

2ZZ also experienced the similar accumulating process. In the early stage (0.5 h) of magnetron sputtering, the ZnO outer layers on the ZnO nanorods are not as compressed as 2ZZ, and those ZnO on the top parts are in particles shape as shown in the HRTEM result of 0.5ZZ (0.5 h decorated ZNRs by ZnO) (Figure S1 in the supporting Information). The distance between the regular lattice planes of the ZnO outer layers is 0.26 nm, corresponding to the interspacing of the (002) planes of wurtzite ZnO, suggesting the *c*-axis texture which is on good agreement with the XRD result (discussed thereafter).

3.2 Crystal structure

XRD was applied to reveal the crystal structures of the nanoarrays. Compared with the XRD pattern of ZNRs grown from hydrothermal method²⁶, no significant difference can be found for 2TZ, 4TZ and 2ZZ as shown in Figure 3. The dominated (002) peak for all samples is indexed to a typical hexagonal wurtzite ZnO crystal structure, which also indicates that the ZnO nanorods have a preferential growth along *c*-axis in [0001] orientation. No obvious peaks of TiO₂ crystal could be noticed for TiO₂/ZnO nanoarrays, which would because the total amount of TiO₂ is very little compared with ZnO matrix. The overwhelming (002) peak and the little peak at 36.2° for 2ZZ imply that the ZnO outer layers deposited by sputtering have a strong *c*-axis texture and some (101) phases.

Interestingly, when we used the fixed position-sensitive detectors (PSD) mode to give a fine X-ray scan (Bruker D2 phaser) between 23° to 28° on 2TZ and 4TZ, a peak at 25.3° was detected for 4TZ, but no such a peak can be captured for 2TZ due to the very limited amount of the TiO₂ outer layers (Figure 4). This peak is indexed to the anatase TiO₂ (101) phase, which means the TiO₂ outer layers were crystallized. The anatase TiO₂ phase of 4TZ can be verified by Raman scattering. The Raman spectrum of 4TZ gives five Raman active fundamental vibrational modes (E_g, E_g, B_{1g}, B_{1g}/A_{1g}, and E_g) of tetragonal anatase structured TiO₂^{27, 28} and one characteristic E₂ mode of wurtzite ZnO.^{29, 30} (Figure S2 in the supporting Information)

The electronic states of the element Ti of 4TZ were analyzed by XPS. Figure 5 shows the fine scan spectrum of Ti 2p. The binding energies of Ti 2p region exhibit two peaks at 464 eV and 458.3 eV, corresponding to Ti 2p_{1/2} and Ti 2p_{3/2}, respectively, indicating the presence of Ti⁴⁺ in the TiO₂ lattice.

3.3 TEM analysis

The detailed morphology and crystal structures of the ZnO based nanoarrays were investigated by TEM and HRTEM as shown in Figure 6. ZnO nanorods are straight with a uniform diameter (60-80 nm) along the entire length, indicating that the anisotropic growth along the *c* axis was perfectly preserved during the growth process (Fig. 6a). It also implies that the growth of ZnO nanorods has great crystal orientation.^{31, 32}

The bush-like TiO₂ layers on the surface of ZnO nanorods make the 4TZ into a core-shell cotton swab-like structure (Fig. 6b-c). The distances between the lattice planes of the TiO₂ part were measured to be 0.35 nm and 0.32 nm, corresponding to the interspacing of the (101) planes of anatase TiO₂ and (110) planes of rutile TiO₂, respectively (Fig. 6d). The selected area diffraction (SAED) pattern of the TiO₂ outer layers displays a polycrystalline

diffraction with a certain concentric rings, indexing to several phases of anatase and rutile TiO₂ (Fig. 6e). The HRTEM image and SAED pattern of 4TZ signify that the TiO₂ outer layers have polycrystalline phases including both anatase and rutile crystals.

The TEM image of 2ZZ is in accordance with the SEM result that the top part of the ZnO nanorod core was accumulated by ZnO crystals into a lollipop-like bi-level structure (Fig. 6f). The ZnO outer layers show some (101) phases of wurtzite ZnO with an interplanar space of 0.25 nm (Fig. 6g).

3.4 Wettability study

The variation on the surface wettability of ZnO based nanoarrays was monitored via water contact angles during their storage times. As displayed in Figure 7, the surface of ZNRs was hydrophilic initially because the contact angle (CA) was 10° when it was measured on the day they were prepared. The surface of ZNRs became hydrophobic after storing in ambient condition for 60 days as the CA increased to 113°. The CA was kept increasing gradually and reached to 145° after over 11 months.

Figures 8 and 9 demonstrate the surface wettability conversion of the TiO₂/ZnO nanocomposite arrays. The as prepared 2TZ also had a hydrophilic surface since the CA was 19° in the beginning and the CA increased slowly to 96° after 264 days and observed as 116° when they were stored for more than 21 months. From hydrophilicity to hydrophobicity, it took longer time than ZNRs for 2TZ and the change rate of CA was slower than ZNRs. The surface wettability of 4TZ experienced the similar trend as 2TZ, but the variation was even slower. It was after 339 days that the 4TZ changed to hydrophobic (CA changed from 12° to 96°), and after more than 21 months, the CA became 106°.

2ZZ, however, exhibited a rather smooth wettability change (Figure 10). The surface had a quite high CA (72°) at the early stage and enlarged very slightly until 105° after over two years. Although it changed from hydrophilic to hydrophobic as ZNRs, 2TZ and 4TZ, the extent was much smaller than the other samples.

During the dark storage in ambient conditions, no intentional modification or chemical treatment was applied to the samples, so their surface geometric microstructure and inherent element nature remain unaltered. We assumed that this conversion on the wettability of the ZnO based nanoarrays is attribute to two kind of changes on the surface: the reduction of hydroxyl groups and the adsorption of organic contaminants.

Because of the nature of semiconductors (ZnO or TiO₂), the surface of the as-prepared nanoarrays are terminated with hydroxyl groups present for the charge neutralization.¹³ The hexagonal wurtzite structure of the ZnO nanorods are composed of polar top surfaces and nonpolar side surfaces. On the nonpolar planes, an equal number of oxygen and zinc ions are terminated in the same face, but the polar surface is dominated by Zn⁺ ions.³³ Since surface oxygen ions are considered to act as reactive sites for attracting OH species, the nonpolar side facets are generally terminated with hydroxyl groups. The hydroxyl groups on the surface are known to have a hydrophilic nature and they can facilitate the imbibing of water droplets via a 3D capillary effect into the nanostructure network, showing the low CA and hydrophilic surface.^{8, 12, 33}

A surface rich in hydroxyl groups is energetically unstable, whereas oxygen adsorption is thermodynamically preferred to

replace the hydroxyl groups when the surface is exposure to an atmosphere containing a higher oxygen partial pressure (in either the air or pure oxygen).^{20, 25} On the losing of the hydroxyl groups, the capillary effect will be weakened. When air becomes trapped within the topographical network, it will act like a cushion and prevent water from seeping into the free space, making the CA higher than before.

On the other hand, the surface would attract amphiphilic contaminants or organic molecules contained in the air gradually during the storage,^{20, 34} which also contribute to the hydrophobicity since they would lower the surface free energy. The effect of the hydroxyl groups and contaminants on the CA of ZnO nanorods and TiO₂/ZnO nanocomposites was illustrated in Figure 11.

The change rates of the wettability of the ZnO based nanoarrays are in the sequence of ZNRs > 2TZ > 4TZ > 2ZZ, which would be ascribed to their microstructure and morphology. The morphology of the nanoarrays differs the surface area and further affects the surface absorbed chemicals (dehydroxylation and contaminant adsorption).

For 2TZ, 4TZ and 2ZZ, the gaps among the nanostructures were obstructed by the out layers of TiO₂ or ZnO, which will decrease the velocity of the replacement of hydroxyl groups by oxygen on the side surfaces of the ZnO nanorods. The bush-like TiO₂ outer layers not only provide more local contact area for water droplets, but also contain interstices to support the capillary effect for the liquid wicking. Besides, as a similar semiconductor as ZnO, TiO₂ is naturally hydrophilic and dominated by hydroxyl groups. Consequently, the OH species on the TiO₂ outer layers and their structural features would also delay the hydrophobicizing rates of 2TZ and 4TZ (Figure 11).

From 2TZ to 4TZ and to 2ZZ, the outermost surface of the nanoarrays becomes more and more flat as the result of longer time sputtering deposition and better matching of the ZnO layers on the ZnO top surfaces, therefore less reactive sites can be attached by organic molecules would be available. In this case, the smoother the outermost surface is, the longer time the wettability conversion would be. Moreover, the very even surface of 2ZZ leads to the high initial CA (72°) due to the limited contact areas and the lack of capillary effect.

To prove the effect of the oxygen absorption on the surface wettability, we placed the fresh ZNRs in a tube furnace under O₂ stream at a low flow rate (25 sccm) to eliminate the influence of other gas components and certain contaminants in the ambient air, and the whole set was maintained at 80°C to accelerate the dehydroxylation process. The surface changed to hydrophobic significantly only in 7 days as the CA increased to 110° and further reached to 126° after 14 days (Figure S3 in the supporting Information). This result indicated that the wettability conversion is largely ascribed to the reduction of hydroxyl groups on the surface.

We soaked hydrophobic ZnO based nanoarrays after long time storage in acetone for 45 h to verify the adsorption of organic molecules on the surface. They all became hydrophilic when they were dried and tested immediately as their CAs decreased from over 100° to less than 80° (65° for ZNRs, 63° for 4TZ and 77° for 2ZZ; Figure S4 in the supporting Information). It is believed that the acetone can dissolve many organic chemicals, hence, the loss

of the adsorbed contaminants would lead to the hydrophilicity. The higher resultant CA of 2ZZ would be resulted from the flatter surface feature.

When the long-time stored samples were treated by ethanol, the hydrophilic conversion was more dramatic even though they were only soaked for 22h. The resultant CAs were 22° for ZNRs, 23° for 4TZ and 73° for 2ZZ when they were dried and tested immediately. (Figure S5 in the supporting Information). The ethanol not only dissolves some organic compounds, but also provides a large amount of extra hydroxyl groups to the surface, confirming the critical role of hydroxylation and contaminants in the wettability transition.

We could imagine that if the as-prepared ZnO based nanoarrays were stored in a circumstance lack of oxygen and organic species, such as in vacuum, from the beginning, the surface wettability will not be influenced by exterior matters and their initial hydrophilic states will last for a longer time.

4. Conclusion

To conclude, the wurtzite ZnO nanorod arrays were synthesized by an aqueous solution method. On the basis of ZnO array matrixes, the TiO₂/ZnO and ZnO/ZnO nanostructure arrays were realized by magnetron sputtering. The TiO₂/ZnO heterostructures are composed of the ZnO nanorod backbones with fluffy TiO₂ outer layers. The ZnO/ZnO nanoarrays have a bi-level structure with compact ZnO outer layers attached on the upper part of the ZnO nanorods.

The surface wettability of these ZnO based nanoarrays transformed spontaneously from hydrophilic to hydrophobic under the ambient atmosphere during long time storage. This is attributed to the replacement of the initial surface hydroxyl groups by oxygen atoms and the adsorption of contaminants in the air. The different wettability change rates of the ZnO based nanoarrays were related to their topographic features and surface chemical components. The abundant open gaps in the ZnO nanorod arrays lead to the rapidest conversion. The flattest ZnO/ZnO nanoarrays experienced the least significant variation and the TiO₂ outer layers delayed the changes of surface hydrophilic property.

This research revealed how the ambient conditions can affect the surface wetting behavior during a long time, and may shed new light on the design of the storage and package of the semiconductor nanodevices.

Acknowledgement

The authors gratefully appreciate the assistance from staff members in the Department of Chemical and Materials Engineering and the Research Centre for Surface and Materials Science at the University of Auckland, especially Ms. Catherine Hobbis, Ms. Laura Liang and Dr. Alec Asadov. The authors would also like to thank the financial support of CSC scholarship.

Notes and references

^a Department of Chemical and Materials Engineering, the University of Auckland, Private Bag 92019, Auckland 1142, New Zealand. Fax: +64 9 3737463; Tel: +64 9 3737599 ext. 89840; E-mail: yliu403@aucklanduni.ac.nz

- ^b School of Materials Science and Engineering, Beijing Institute of Technology, Beijing 100081, China
- [†] Electronic Supplementary Information (ESI) available: HRTEM images of 0.5ZZ. Raman spectrum of 4TZ. CA of ZNRs after O₂ treatment for (a) 7 days and (b) 14 days. CA of (a) ZNRs, (b) 4TZ and (c) 2ZZ after soaking in acetone for 45h. CA of (a) ZNRs, (b) 4TZ and (c) 2ZZ after soaking in ethanol for 22h. See DOI: 10.1039/b000000x/
1. J. G. Lv, J. B. Zhu, K. Huang, F. M. Meng, X. P. Song and Z. Q. Sun, *Appl. Surf. Sci.*, 2011, **257**, 7534-7538.
 2. P. H. Yang, K. Wang, Z. W. Liang, W. J. Mai, C. X. Wang, W. G. Xie, P. Y. Liu, L. Zhang, X. Cai, S. Z. Tan and J. H. Song, *Nanoscale*, 2012, **4**, 5755-5760.
 3. R. N. Wenzel, *Industrial and Engineering Chemistry*, 1936, **28**, 988-994.
 4. R. N. Wenzel, *Journal of Physical and Colloid Chemistry*, 1949, **53**, 1466-1467.
 5. X. J. Feng and L. Jiang, *Adv. Mater.*, 2006, **18**, 3063-3078.
 6. Z. Guo, X. Chen, J. Li, J. H. Liu and X. J. Huang, *Langmuir*, 2011, **27**, 6193-6200.
 7. L. Zheng, Z. Li, S. Bourdo, V. Saini, C. Ryerson and A. S. Biris, *ChemPhysChem*, 2011, **12**, 2412-2414.
 8. G. Kwak, S. Jung and K. Yong, *Nanotechnology*, 2011, **22**.
 9. Y. Li, M. Zheng, L. Ma, M. Zhong and W. Shen, *Inorg. Chem.*, 2008, **47**, 3140-3143.
 10. X. J. Feng, S. C. Roy and C. A. Grimes, *Langmuir*, 2008, **24**, 3918-3921.
 11. X. X. Zhang, L. Wang and E. Levanen, *RSC Adv.*, 2013, **3**, 12003-12020.
 12. S. B. Kim, W. W. Lee, J. Yi, W. I. Park, J. S. Kim and W. T. Nichols, *ACS Appl. Mater. Interfaces*, 2012, **4**, 3910-3915.
 13. C. Mondal, M. Ganguly, A. K. Sinha, J. Pal and T. Pal, *RSC Adv.*, 2013, **3**, 5937-5944.
 14. A. Ramirez-Canon, D. O. Miles, P. J. Cameron and D. Mattia, *RSC Adv.*, 2013, **3**, 25323-25330.
 15. V. A. Ganesh, S. S. Dinachali, H. K. Raut, T. M. Walsh, A. S. Nair and S. Ramakrishna, *RSC Adv.*, 2013, **3**, 3819-3824.
 16. W. T. Sun, S. Y. Zhou, P. Chen and L. M. Peng, *Chem. Commun. (Cambridge, U. K.)*, 2008, 603-605.
 17. U. Ozgur, Y. I. Alivov, C. Liu, A. Teke, M. A. Reshchikov, S. Dogan, V. Avrutin, S. J. Cho and H. Morkoc, *J. Appl. Phys.*, 2005, **98**.
 18. A. McLaren, T. Valdes-Solis, G. Li and S. C. Tsang, *J. Am. Chem. Soc.*, 2009, **131**, 12540-12541.
 19. V. Khranovskyy, T. Ekblad, R. Yakimova and L. Hultman, *Appl. Surf. Sci.*, 2012, **258**, 8146-8152.
 20. R. D. Sun, A. Nakajima, A. Fujishima, T. Watanabe and K. Hashimoto, *J. Phys. Chem. B*, 2001, **105**, 1984-1990.
 21. X. Zhu, Z. Zhang, X. Men, J. Yang and X. Xu, *Appl. Surf. Sci.*, 2010, **256**, 7619-7622.
 22. J. Li, H. Q. Wan, X. H. Liu, Y. P. Ye, H. D. Zhou and J. M. Chen, *Appl. Surf. Sci.*, 2012, **258**, 8585-8589.
 23. E. L. Papadopoulou, A. Pagkozidis, M. Barberoglou, C. Fotakis and E. Stratakis, *J. Phys. Chem. C*, 2010, **114**, 10249-10253.
 24. J. Zhang, Y. R. Liu, Z. Y. Wei and J. Y. Zhang, *Appl. Surf. Sci.*, 2013, **265**, 363-368.
 25. X. Feng, L. Feng, M. Jin, J. Zhai, L. Jiang and D. Zhu, *J. Am. Chem. Soc.*, 2003, **126**, 62-63.
 26. Y. S. Liu, J. Han, W. Qiu and W. Gao, *Appl. Surf. Sci.*, 2012, **263**, 389-396.
 27. W. F. Zhang, Y. L. He, M. S. Zhang, Z. Yin and Q. Chen, *J. Phys. D- Appl. Phys.*, 2000, **33**, 912-916.
 28. H. Cheng, J. Ma, Z. Zhao and L. Qi, *Chem. Mater.*, 1995, **7**, 663-671.
 29. P. Jiang, J. J. Zhou, H. F. Fang, C. Y. Wang, Z. L. Wang and S. S. Xie, *Adv. Funct. Mater.*, 2007, **17**, 1303-1310.
 30. S. S. Kanmani and K. Ramachandran, *Renewable Energy*, 2012, **43**, 149-156.
 31. H. Yu, Z. Zhang, M. Han, X. Hao and F. Zhu, *J. Am. Chem. Soc.*, 2005, **127**, 2378-2379.
 32. Y. Liu, Y. Chu, L. L. Li, L. H. Dong and Y. J. Zhuo, *Chem.--Eur. J.*, 2007, **13**, 6667-6673.
 33. P. Colson, A. Schrijnemakers, B. Vertruyen, C. Henrist and R. Cloots, *J. Mater. Chem.*, 2012, **22**, 17086-17093.
 34. T. J. Wood, G. A. Hurst, W. C. E. Schofield, R. L. Thompson, G. Oswald, J. S. O. Evans, G. J. Sharples, C. Pearson, M. C. Petty and J. P. S. Badyal, *J. Mater. Chem.*, 2012, **22**, 3859-3867.

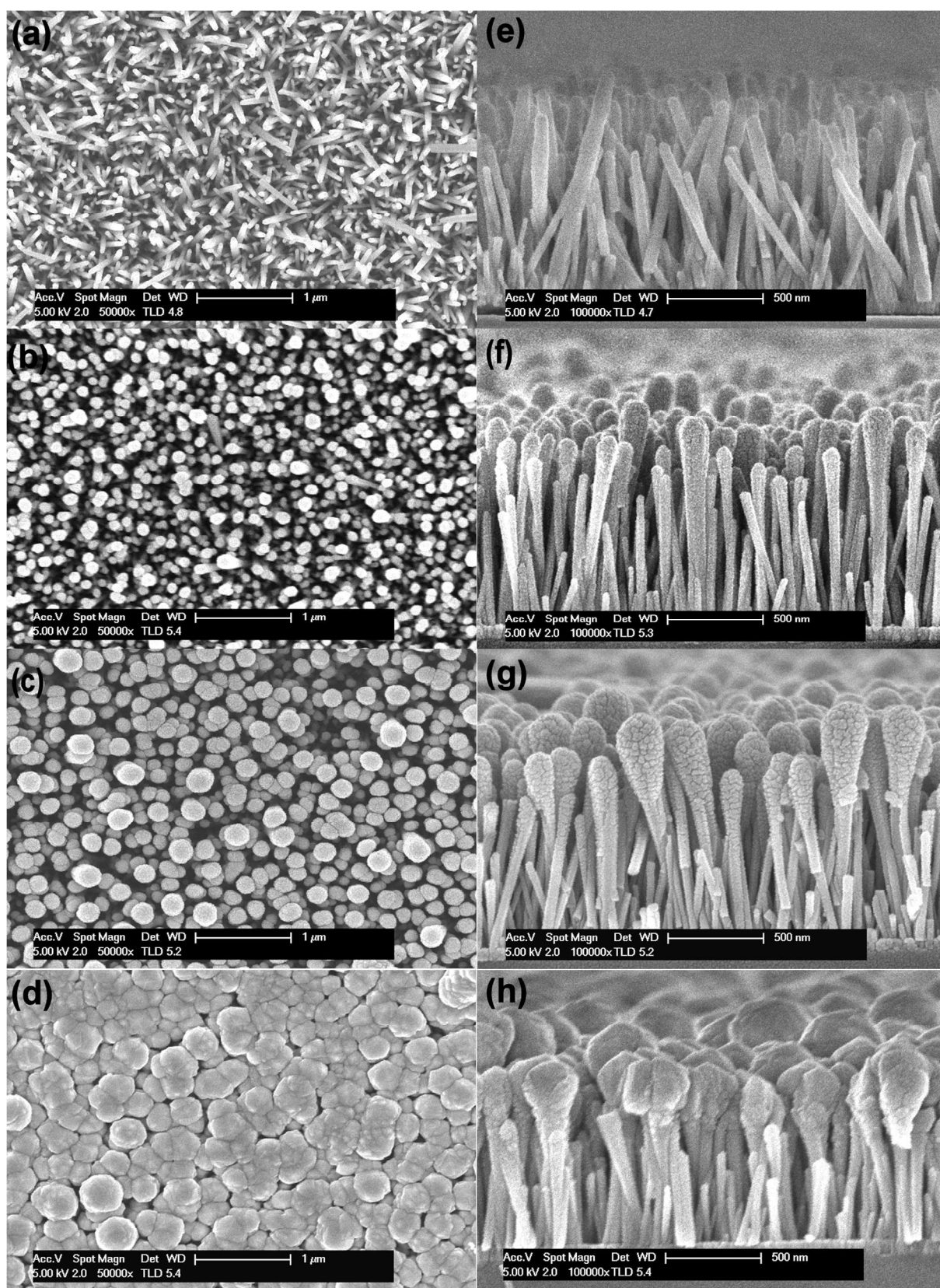


Fig. 1 SEM images of (a-d) top section and (e-h) cross section of ZNRs, 2TZ, 4TZ and 2ZZ.

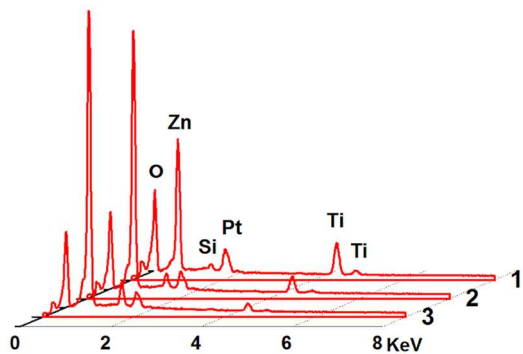
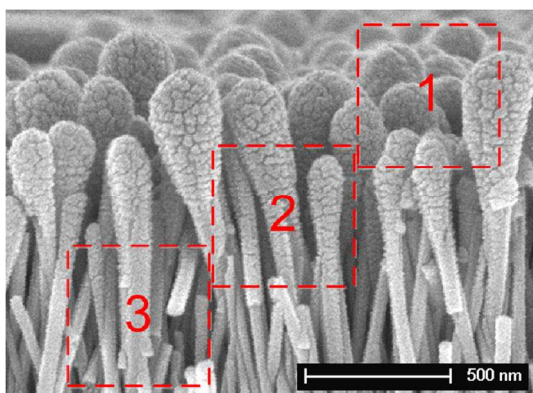


Fig. 2 EDS spectra from the adjacent areas along the cross section of 4TZ.

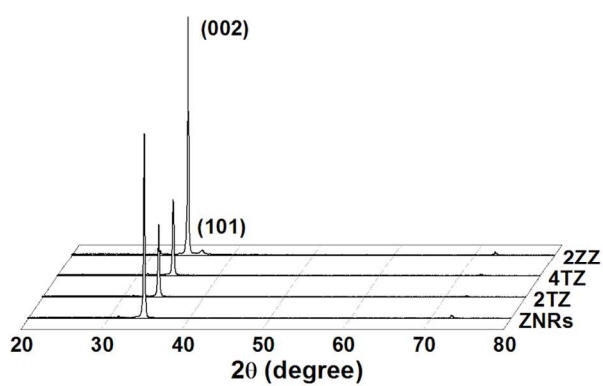


Fig. 3 XRD patterns of ZNRs, 2TZ, 4TZ and 2ZZ.

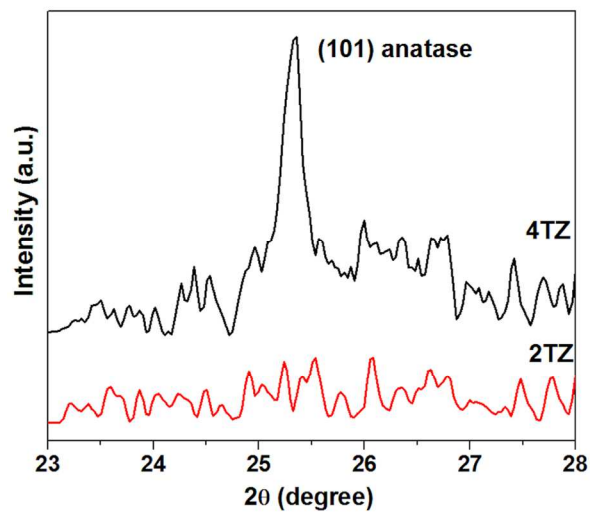


Fig. 4 XRD patterns between 23° to 28° of 4TZ 2TZ and 4TZ.

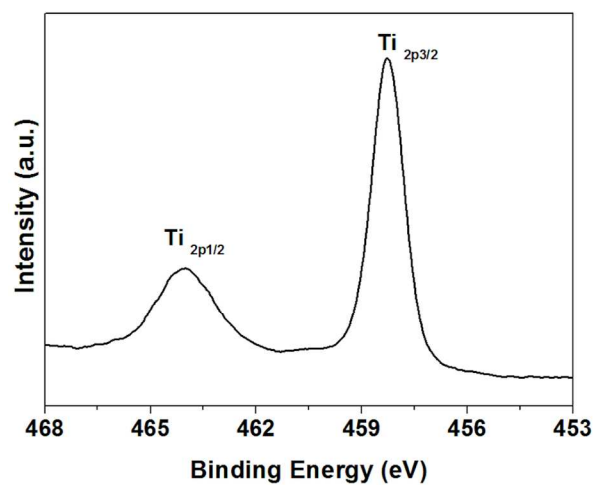


Fig. 5 High resolution XPS spectrum of Ti 2p of 4TZ.

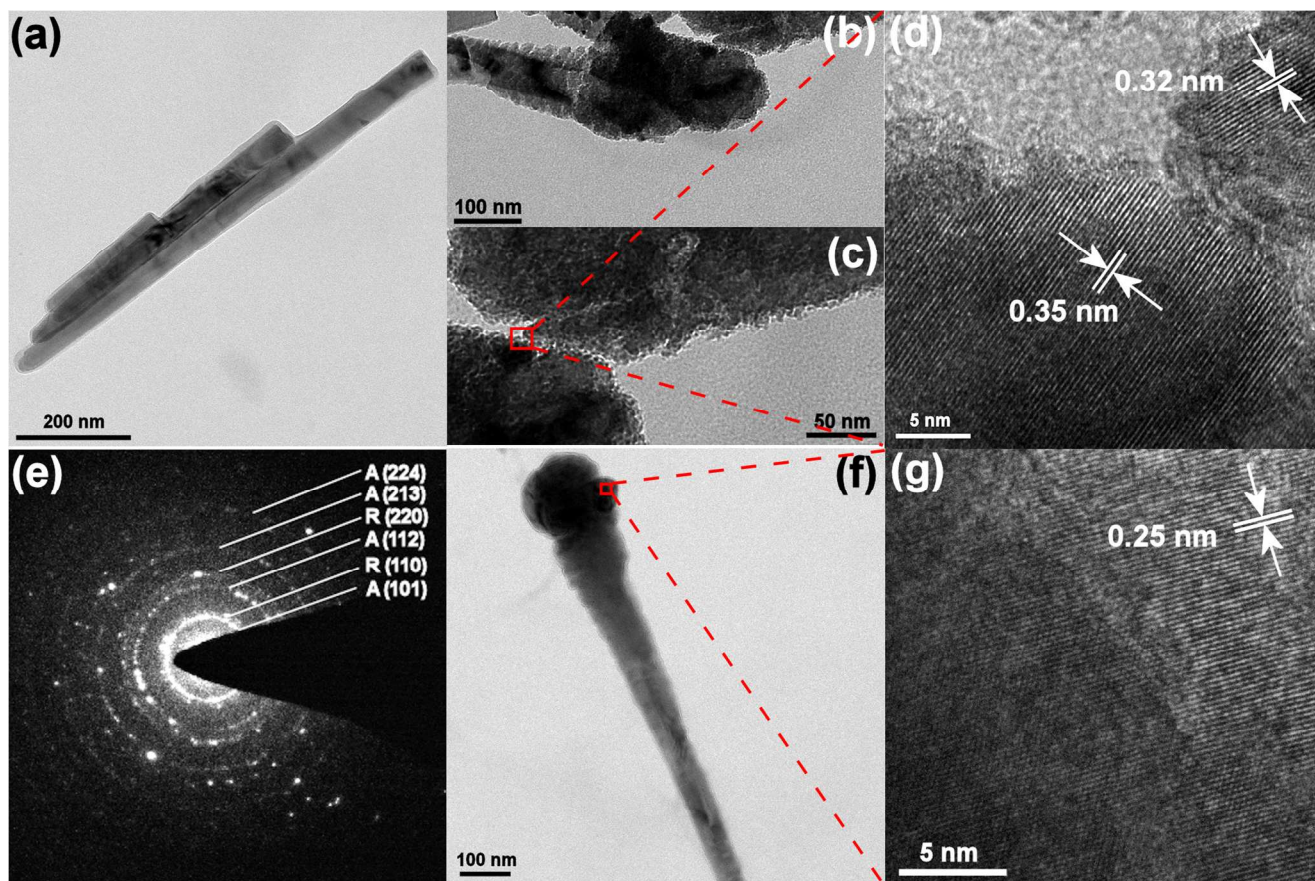


Fig. 6 (a) TEM image of ZNRs; (b-c) TEM images of 4TZ; (d) HRTEM image of TiO₂ outer layers of 4TZ; (e) SAED pattern of the TiO₂ outer layers; (f) TEM image of 2ZZ; (g) HRTEM images of ZnO outer layers of 2ZZ.

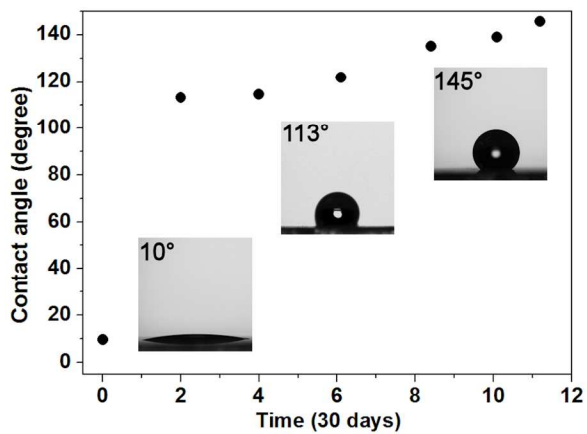


Fig. 7 Wettability conversion of ZNRs during the storage in ambient conditions.

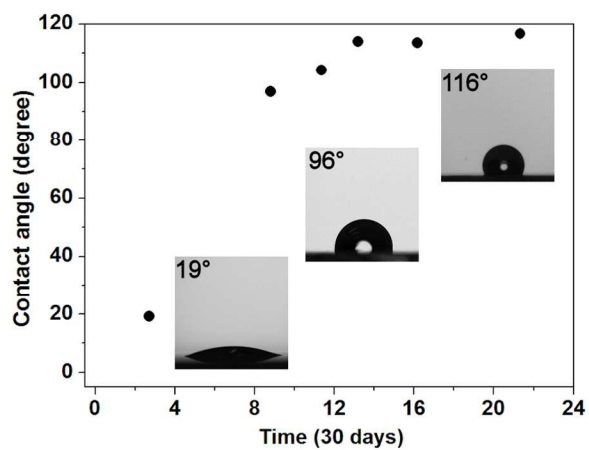


Fig. 8 Wettability conversion of 2TZ during the storage in ambient conditions.

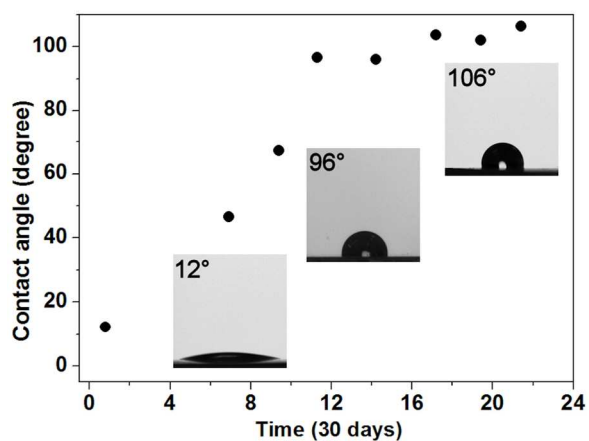


Fig. 9 Wettability conversion of 4TZ during the storage in ambient conditions.

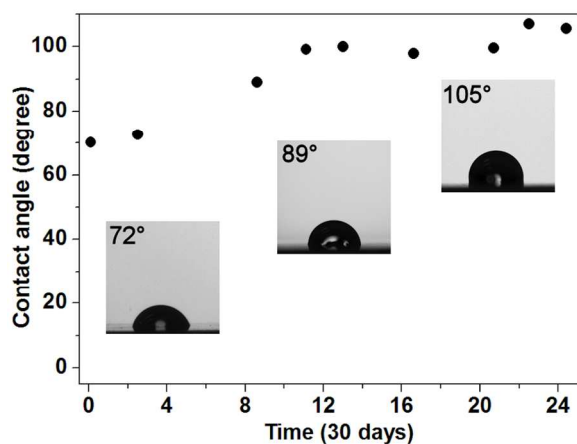


Fig. 10 Wettability conversion of 2ZZ during the storage in ambient conditions.

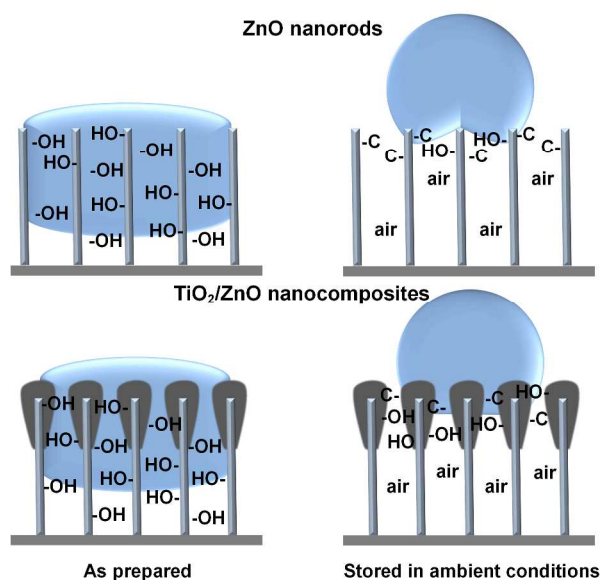


Fig. 11 Schematic models of the water contact angle on the surface of ZnO nanorod and TiO₂/ZnO nanocomposite arrays when they were produced and after a certain time storage in ambient conditions (-OH: hydroxyl group; -C: contaminant).